

Comparing Mechanical and Corrosion Behaviour of TIG & FSW Weldments of AA5083-H321

Harinder Singh Grover^{1*}, Vikas Chawla¹ and Gurbhinder Singh Brar²

¹IK Gujral Punjab Technical University, Jalandhar - 144603, Punjab, India; harinder28@gmail.com, vikas.chawla.ikgptu@gmail.com

²Guru Kashi University, Talwandi Sabo - 151302, Punjab, India; gurbhinder@yahoo.com

Abstract

Objective: To study the influence of tungsten inert gas welding and friction stir welding on the mechanical properties and corrosion behaviour of AA5083-H321 weldments. **Methodology:** The received AA5083-H321 5 mm thick plates were welded by Tungsten inert gas welding (TIG) and friction stir welding (FSW) at optimized process parameters discovered in previous research work. Corrosion tests ASTM G66 and ASTM G67 as specified by ASTM 928M standards for marine service was performed for study the corrosion behaviour of the weld joints. **Findings:** It was found that TIG weldments are more susceptible to exfoliation and intergranular corrosion than FSW weld samples, and parent substrate. **Novelty/Improvement:** The adoption of friction stir welding in ship building industries can further reduce the corrosion occurred in ship structures in service.

Keywords: AA5083-H321, ASTM G66, ASTM G67, Exfoliation Corrosion, Intergranular Corrosion

1. Introduction

The Al-Mg alloys of 5xxx series are widely deployed in transport industry particularly ship building industry due to having high strength to weight ratio, excellent formability, and ease in welding, and favourable corrosion resistance to seawater and marine atmosphere. Among the 5xxx aluminum alloy series, AA5083 alloy is most often used in shipbuilding with specified tempers H116 (strain hardened) and H321 (thermally stabilized) under ASTM B928M standard for "High Magnesium Aluminium alloy sheet & plate for marine Service" for continuous services under operating temperatures less than 66 °C¹.

The AA5083 aluminium alloy as a major shipbuilding material has appealed significant research attention to study the weld ability of it. The TIG and GMAW joints of AA5083 were compared and was discovered that the welded joints with gas tungsten arc welding are more mechanically reliable than gas metal arc welded joints².

Partial penetration laser welding on AA5083-H321 was performed to investigate the effects of process parameters³. The comparison of mechanical properties of AA5083-H321 weldments joined by TIG welding and laser beam welding concluded that laser beam welding gives superior mechanical properties than TIG welding⁴. The weld ability of the aluminum alloy AA5083 with a high power diode laser welding was investigated⁵.

Many researchers inspected the influence of process parameters of friction stir welding on mechanical properties, microstructures and fatigue life for AA5083 aluminium alloy. It was discovered that grain size in nugget zone is directly proportional to friction heat flow while studying the effect of process parameters of friction stir welding on AA5083-O⁶. Investigations were done to study the effect of tool rotational speed and welding speed on mechanical properties and fatigue life of AA5083-H321 friction stir weldments⁷. The optimization of process parameters of friction stir welding of AA5083-H111 by

*Author for correspondence

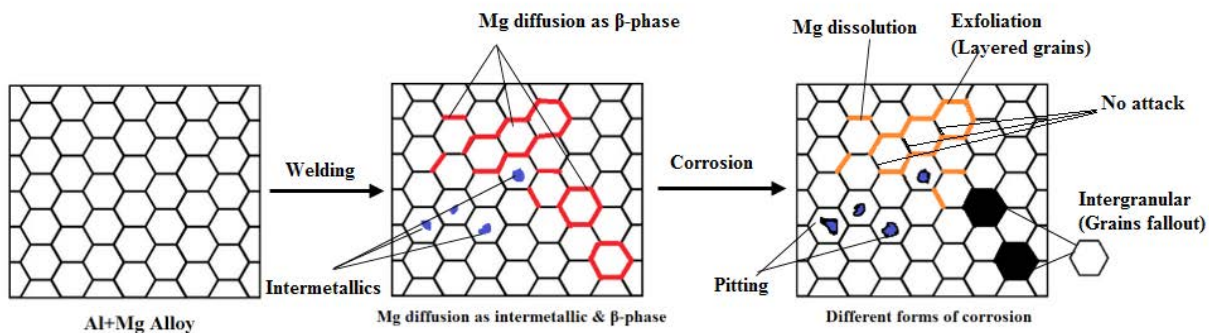


Figure 1. Corrosion behaviour of Al-Mg alloys.

utilizing response surface methodology was successfully carried out⁸.

Although Al-Mg alloys are continually deployed in marine services, the disturbing issue is the marine corrosion. The susceptibility to stress corrosion cracking, pitting corrosion, exfoliation and intergranular corrosion increases for the aluminium Mg alloys having Mg content > 3% weight when exposed to higher temperatures (>50 °C) for longer service conditions⁹. A general overview of possible types of corrosion behaviour (pitting, intergranular, exfoliation) of Al-Mg alloys has been shown in Figure 1.

Marine corrosion causes the deterioration of structures and vessels immersed in seawater, the corrosion of machinery and piping systems that use seawater for cooling and other industrial purposes, and corrosion in marine atmosphere¹⁰. Corrosion of the built structures due to marine salts in coast areas has been a major and continuing problem and adversely affects the robustness of the structures and reducing their service life¹¹. The seawater is a severe environment in which the materials can be attacked by pitting and crack corrosion¹².

ASTM G66 and ASTM G67 corrosion tests were performed on friction stir welded AA5083-H111 and was shown that the parent metal was more sensitive to intergranular corrosion than welded zone¹³. AlMg6Mn alloy was reported to be more susceptible to intergranular corrosion than TIG weldments and both were insensitive to exfoliation corrosion¹⁴. The comparison of FSW and MIG weldments of AA5083 alloy for pitting and stress corrosion cracking (SCC) revealed that FSW technique had higher corrosion resistance¹⁵.

Although mechanical properties of AA5083-H321 joints welded by friction stir welding were investigated by several researchers¹⁶⁻¹⁸, a little research work has been carried out for studying the corrosion behaviour of weldments of AA5083-H321. This research work has been carried out to study and compare the corrosion behaviour of fusion welding and friction stir welding of AA5083-H321. For comparison, the FSW and TIG joints with maximum mechanical properties were selected from the previous research work carried out by the authors. ASTM G66-99 and ASTM G67-13 corrosion test were performed to study the corrosion behaviour of weldments.

Table 1. Chemical composition and mechanical properties of AA5083-H321

AA5083-H321 Aluminum Alloy Chemical Composition							Mechanical Properties				
Cu	Mg	Si	Fe	Mn	Zn	Cr	Ti	Al	UTS (MPa)	Impact Toughness (J)	Hardness (HV)
0.0016	4.296	0.14	0.059	0.731	0.008	0.135	0.014	Bal	320	21	101

Table 2. Optimized process parameters of FSW and TIG welding

FSW process parameters	Value	TIG	Value
Tool rotational speed (RPM)	830	Current (amp)	200
Welding speed (mm/min.)	48	Welding speed (mm/min.)	40
Plunge depth (mm)	0.07	Gas flow rate (L/min.)	10
Tool pin profile	Taper Hexagonal		

2. Experimental Work

2.1 Material Selection

The substrate selected in research work was 5083-H321 aluminum alloy and was procured in plate form (8ft. X 6ft.) with thickness of 5 mm. The plates of size 300 X 100 mm were cut by shearing machine and milling. The analyzed chemical composition and mechanical properties of the base metal are tabulated in Table 1.

2.2 Welding of AA5083-H321

In previous researches, carried out by the authors themselves, friction stir welding and tungsten inert gas welding of 5 mm thick plate of AA5083-H321 was performed as per design matrix using response surface methodology (RSM) as a technique for design of experiments. Thirty-one joints were prepared by friction stir welding and twenty joints were prepared by tungsten inert gas welding. After welding, samples were cut for mechanical testing as per ASTM standards using electric discharge cutting machine. Ultimate tensile test, impact test and hardness test at the centre of weld zone were performed. The RSM was used to optimize the process parameters followed by confirmation tests, which gave the satisfactory results and were within the confidence interval of the predicted. The optimized process parameters of both types of welding, resulting in maximum mechanical properties, are given in Table 2.

2.3 Corrosion Testing

The FSW and TIG welded joints having maximum mechanical properties were selected for further corrosion behaviour analysis. ASTM Standard, B928M, was established in 2004 for marine aluminum alloys with the purpose to prevent the use of alloys and tempers that are not resistant to intergranular corrosion, exfoliation and stress corrosion. ASTM B928M¹⁹ implies that marine aluminum alloy products in the 5xxx-H321 and 5xxx-H116 temper meet the resistance to exfoliation corrosion, and intergranular corrosion (IGC), as determined by testing by ASTM G66 (ASSET), and ASTM G67-13 (NAMLT) respectively.

2.3.1 ASTM G66-99 exfoliation corrosion test

Exfoliation corrosion test as per ASTM standard G66-99 were implemented on parent substrate and each sample of the optimized FSW and TIG weldments. The standard

practice is the visual evaluation of exfoliation corrosion susceptibility of AA5XXX (ASSET Test). The codes and classifications used for recording the visual appearance of corroded samples are tabulated in Table 3. Visual ratings of different degrees of pitting or exfoliation may be indicated PA, PB, PC or EA, EB, EC, ED and are given by comparing with standard visual reference photographs²⁰.

Table 3. Codes and classifications for corrosion in ASTM G66-99

Code	Classification
N	No appreciable attack
P	Pitting
E	Exfoliation

The samples of 40 mm x 100 mm x 5 mm were cut from parent substrate, FS and TIG weldments of AA 5083-H321 and were undergone pickling. The samples were immersed in 5% NaOH solution at 80°C for 1min. then for desmuting, the samples were immersed in HNO₃ at room temperature for 30 seconds. After then, the samples were immersed vertically in test solution having the composition of 1.0M ammonium chloride (NH₄Cl), 0.25M ammonium nitrate (NH₄NO₃), 0.01M ammonium tartrate ((NH₄)₂C₄H₄O₆), and 0.09M hydrogen peroxide (H₂O₂) for 24 hours at 65 °C regulated by a heated water bath. After this, the specimens were assessed visually for exfoliation corrosion susceptibility of specimens. SEM analysis of corroded area was also carried out.

2.3.2 ASTM G67-13 intergranular corrosion test

ASTM G67-13²¹ intergranular corrosion test is performed for determining the susceptibility to intergranular corrosion of AA5XXX measuring the mass loss after exposure to nitric acid (NAMLT Test). In this test method, the test samples are immersed in concentrated nitric acid at 30°C for 24 hours. The weight of test specimens is recorded before and after test. The mass loss per unit area defines the measure of susceptibility to intergranular corrosion. Second phase β Al-Mg (aluminum-magnesium intermetallic compound) dissolves in nitric acid in preference to the solid solution of magnesium in the aluminum matrix.

Samples of size 6 mm x 50 mm x 5 mm were cut from parent substrate, FS and TIG weldments of AA 5083-H321 and were undergone pickling. The samples were first immersed in 5% NaOH solution at 80° C for 1 min. Then the samples were desmutted in HNO₃ for 30 seconds

at room temperature. The initial weight of the samples was measured and tabulated in Table 4. After then, the samples were immersed in concentrated nitric acid at 30° C for 24 hours regulated by a heated water bath. After this, the specimens were again weighed for mass loss by intergranular corrosion of specimens (Table 4). It was observed that the loss mass in the parent substrate sample is the least than in both welded samples. SEM and EDS analysis of corroded area was also carried out.

Table 4. Mass loss value for samples in ASTM G67 test

Sample	Weight before (mg)	Weight after (mg)	Mass loss (mg)
Parent substrate	3957.2	3873.2	84
FSW weld	4189.8	4031.4	158.4
TIG weld	4417.3	4080.1	337.2

3. Results and Discussion

3.1 Weld appearance

The weld bead appearance of FSW and TIG weldments are shown in Figure.2(a)-(b). It is clearly shown that the weld bead appearance of FSW weld joint is far better than in case of TIG weld joint.

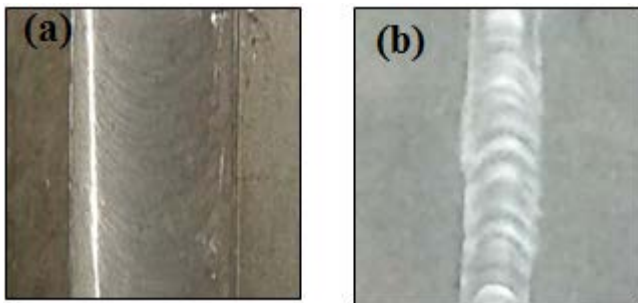


Figure 2. Weld appearance (a) FSW (b) TIG weld.

3.2 Mechanical properties

The mechanical properties; ultimate tensile strength, impact strength and hardness of parent substrate, FSW and TIG weldments are compared in Figure 3. Figure 3(a) shows that the tensile strength of both types of weld joints is inferior to parent substrate. However, FSW weld joint has superior tensile strength (277 MPa) than that of TIG weld joint (231 MPa). There was merely 15% reduction in tensile strength in case of FSW as compared to 28%

reduction in case of TIG weld joints. Figure3(b) shows the comparison of impact strength. Here FSW causes only 14% reduction in impact strength as compared to 23% reduction in case of TIG weld joint.

Figure 3(c) shows the hardness value at the center of the weld zone. The lower values of hardness in TIG weld joint clearly reveal the inferior tensile behavior. The hardness reduction at weld zone at TIG weld joint is 14% as compared to only 1% in case of FSW weld joint.

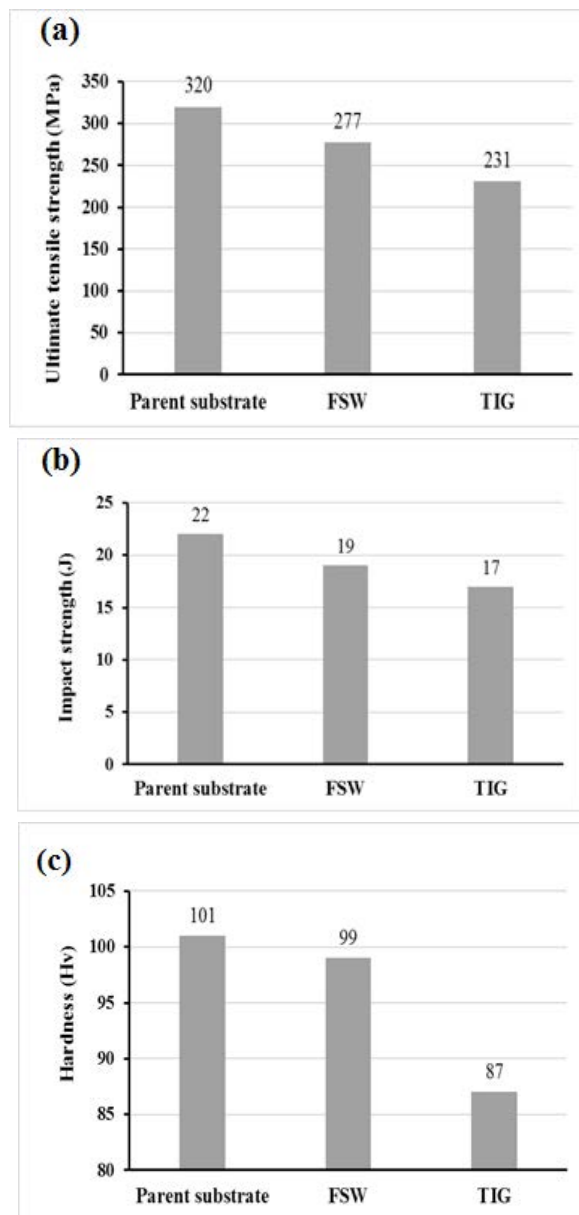


Figure 3. Comparison of mechanical properties of parent substrate, FSW and TIG weld (a) ultimate tensile strength, (b) impact strength (c) hardness.

The Fractography of FSW weld and TIG weld joints is shown in Figure 4. In Figure 4(a), there are fine and uniformly distributed dimples in case of FSW weld and coarser dimples in TIG weld (Figure 4b), which are evident for the tensile behavior of two weld joints being compared. Tensile properties have indirectly proportional relation to dimple size; smaller the dimple size, the tensile strength will be higher and vice versa²². TIG welding process is associated with melting of weld zone and excess heat generation which results in slower cooling rates leading in more softening of material and grain coarsening, resulting in lowering mechanical properties, whereas FSW being solid state welding process, does not melt the weld zone and hence no excess heat is generated and leading to faster cooling rates and finer grain microstructure formation, resulting in better mechanical properties.

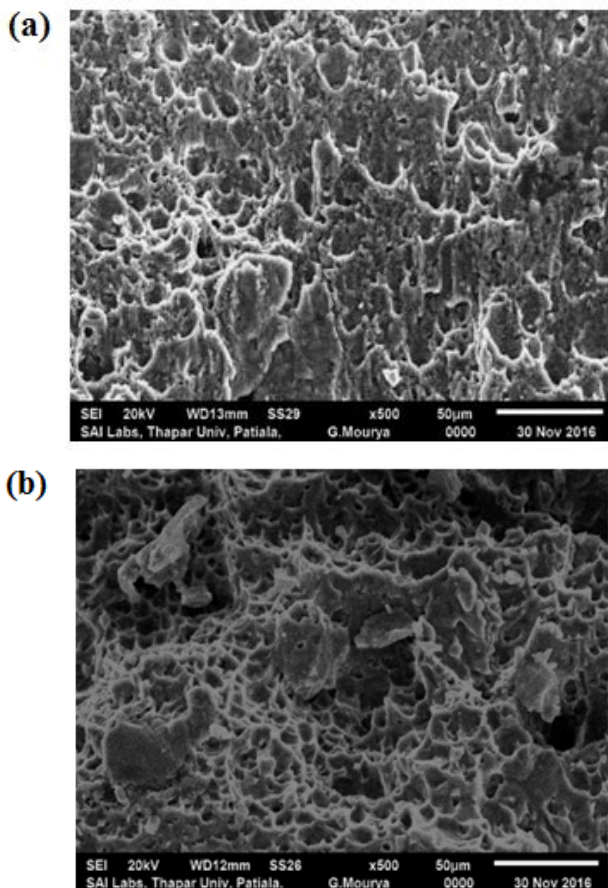


Figure 4. Fractography of (a) FSW weld (b) TIG weld joint.

3.3 Corrosion behavior

Figure 5 shows surface visual appearance and Scanning Electron Microscopy (SEM) morphology of the corro-

sion test samples (parent substrate, FS and TIG weldment zones of AA5083-H321) of the exfoliation corrosion tests (ASTM G66). The parent substrate (Figure 5a) and FS (Figure 5b) weldments have undergone pitting corrosion as compared to exfoliation corrosion in TIG weldment (Figure 5c).

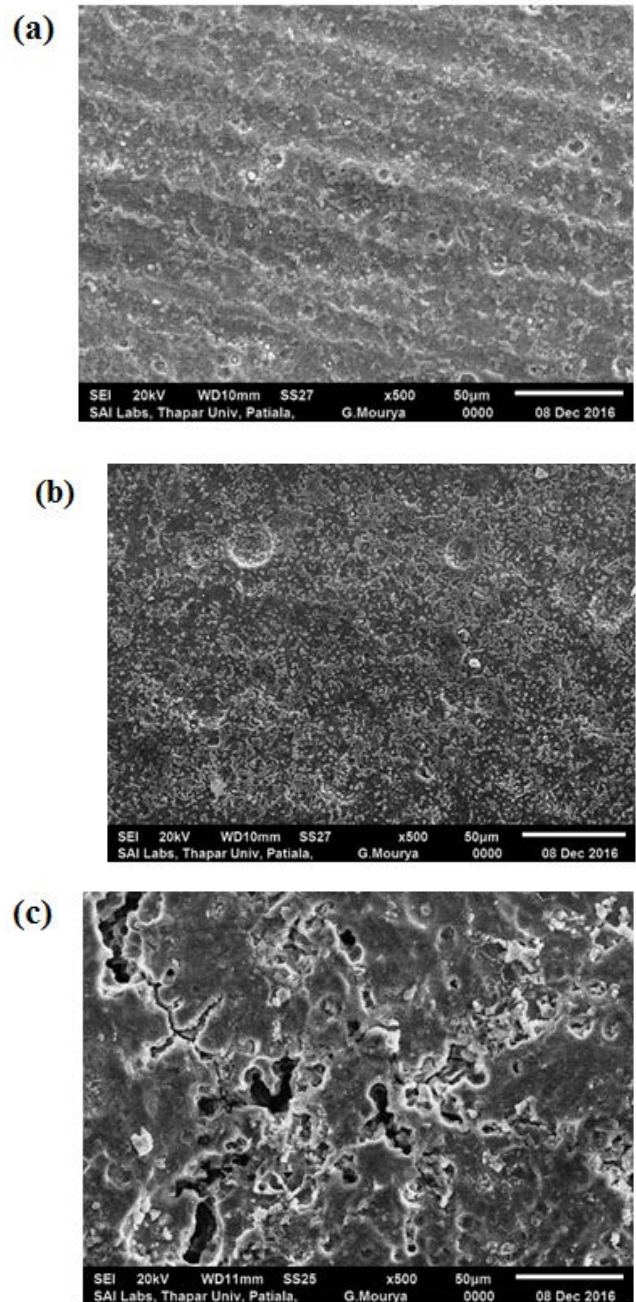


Figure 5. Scanning Electron Microscopy (SEM) morphology of the G66 corrosion test samples (a) parent substrate, (b) Friction stir weld zone (c) TIG weld zone.

The intermetallic particles are supposed to liable for initiation of pitting corrosion due to the variation in the corrosion potential with respect to the aluminum matrix. Based on the corrosion potential of the intermetallic particles, the particles either corrode or promote the surrounding aluminum matrix to dissolve, resulting in a pitting corrosion²³. In the present case of AA5083-H321Mg intermetallic particles act as anode and promote the surrounding aluminum matrix to dissolve. Hence parent substrate experienced the pitting corrosion. In FS weld sample, the intermetallic particle might have had breakdown under the action of rotating tool²⁴, due to which, lesser but uniform pitting corrosion can be seen there.

The higher heat inputs associated with TIG welding as compared to low temperatures in friction stir welding results in coarser grain structures. Also accumulations of magnesium β -phase grow at grain boundaries at elevated temperatures²⁵. Thus continuous precipitation of magnesium β -phase, at the elongated grain boundaries of AA5083-H321 TIG weldments, increases the susceptibility of weldments to exfoliation corrosion. Exfoliation corrosion of metals and alloys is characterized by attack developed preferentially along planes parallel to the working direction. The continuous voids shown in Figure.4 (c) could be the evidence of exfoliation corrosion in case of TIG weld sample.

Figure 6 shows surface visual appearance and Scanning Electron Microscopy (SEM) morphology of the corrosion test samples (parent substrate, FS and TIG weldments of AA5083-H321) of the intergranular corrosion tests (ASTM G67). The parent material (Figure 6a) presents a superior resistance to intergranular corrosion followed by FS (Figure 6b) and TIG weldments (Figure6c). The β -phase at the grain boundaries acts as a catalyst encouraging crack growth and following intergranular corrosion cracking through anodic dissolution²⁶. It can be seen clearly from the SEM images that the most severe attack is on TIG weldments, where large pits of 100 μm size are visible in weld zone, which may be due to the presence of continuous network of β -phase around the grains, which were preferentially dissolved by nitric acid, and causing the grains to fall away from samples, whereas incase of FS weldments the pits of 20 to 30 μm are created, may be due to the breaking up of the coarse particles of the magnesium β -phase into smaller ones by the action of rotating tool. Due to the same reason, the higher popu-

lation density of pits but of small sizes can be seen in FS weldment samples.

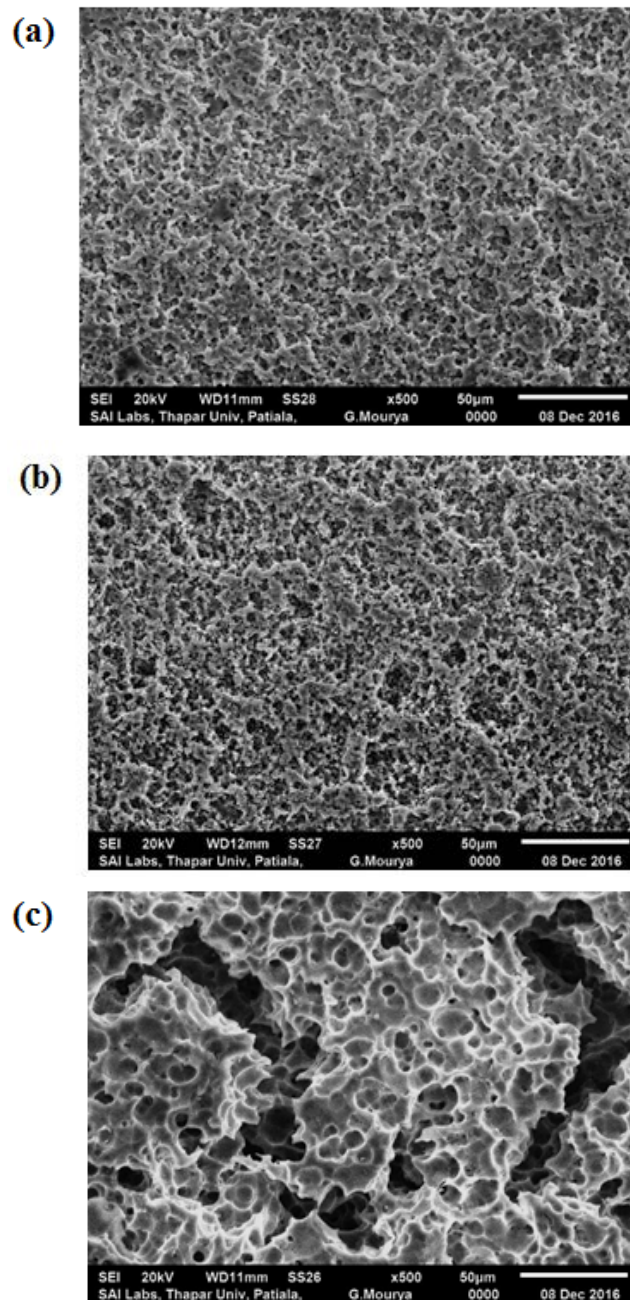


Figure 6. Scanning Electron Microscopy (SEM) morphology of the G-67 corrosion test samples (a) parent substrate, (b) Friction stir weld zone (c) TIG weld zone.

As the Mg intermetallic particles around grain boundaries are attacked and dissolved by nitric acid, therefore minimum Mg weight percentage in EDS analysis of TIG weld sample (Figure7c) as compared to other

corrosion test samples of parent substrate (Figure 7a) and FS weld (Figure 7b), gives strong confirmation that maximum intergranular corrosion has occurred in TIG weld sample.

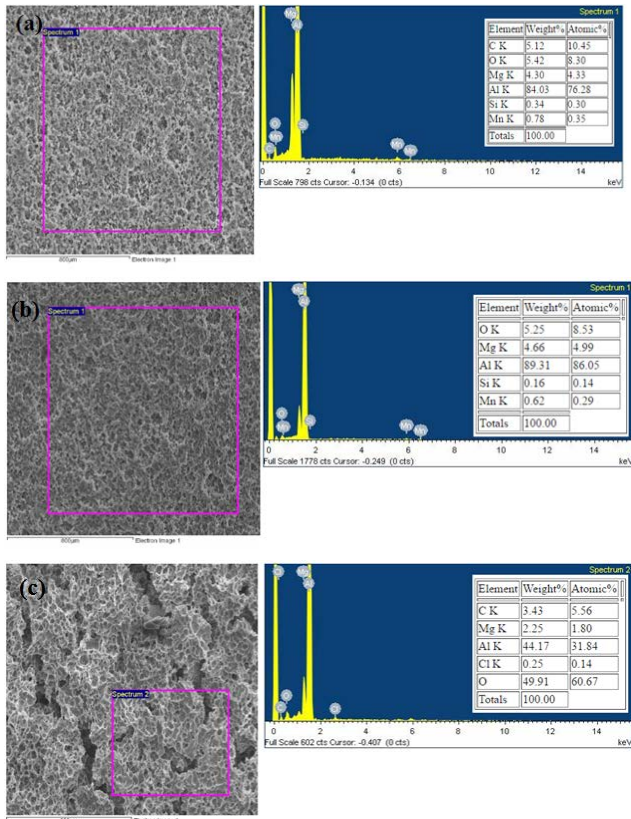


Figure 7. EDS analysis ASTM G67 corrosion test samples (a) parent substrate, (b) Friction stir weld zone (c) TIG weld zone.

Figure 8 shows mass loss value for three samples in the NAMLT. Dotted lines show the classification of degree of sensitization to intergranular corrosion. According to the standards, the alloy is considered resistant to intergranular corrosion when the mass loss per unit area is less than or equal to 15 mg/cm^2 , and if it is greater than or equal to 25 mg/cm^2 , then the alloy is considered susceptible to intergranular corrosion. When the mass loss is between $15\text{--}25 \text{ mg/cm}^2$ the sensitivity to intergranular corrosion is undetermined. It has been observed that the loss of mass in the TIG weld samples (29.07 mg/cm^2) is higher than in the FS welded samples (13.06 mg/cm^2) followed by parent substrate (7.24 mg/cm^2). Thus from it can be concluded that the friction stir welding did not influence the corrosion behavior as compared to TIG welding.

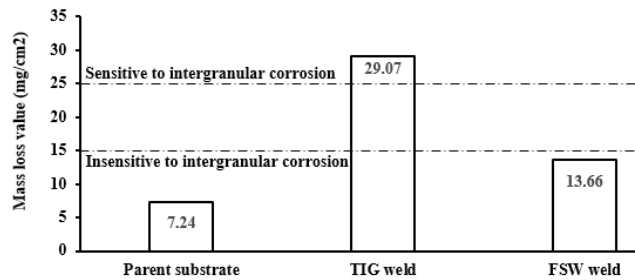


Figure 8. Mass loss value for different Al-Mg alloy samples in the G67-13 test.

4. Conclusion

The friction stir welding performs better in terms of mechanical properties for AA5083-H321 as compared to tungsten inert gas welding.

The susceptibility to intergranular (IGC) and exfoliation corrosion of parent substrate, TIG welded and FSW welded samples of AA5083-H321 alloy at optimized working conditions were investigated according to the ASTM G66 and ASTM G67 standards. From investigations, it was clear that parent substrate was excellent corrosion resistant material and follows ASTM 928M standards for marine services. G66-99 test explored that parent substrate and FS weldments have superior resistance to exfoliation resistance, but are prone to pitting corrosion of low intensity, as compared to exfoliation corrosion occurred on TIG weldments. From the ASTM G67 test, it could be concluded that the TIG weldment of the substrate material failed to follow the ASTM 928M standards as mass loss was 29.07 mg/cm^2 attributed to severe β -phase dissolution in nitric acid and had undergone intergranular corrosion. Whereas friction stir weld showed excellent corrosion resistance to intergranular corrosion, where the mass loss was 13.66 mg/cm^2 , which is considered as a measure to be insensitive to intergranular corrosion as per ASTM G-67 standards. Thus it can be concluded that friction stir welding process can successfully produce the excellent corrosion resistant joints of AA5083-H321 as compared to tungsten inert gas welding.

5. References

- Romhanji E, Popovic M. Problems and prospect of Al-Mg alloys application in marine constructions. *Metalurgija*. 2006; 12(4):297–307.
- Liu Y, Wang W, Xie J, Sun S, Wang L, Qian Y, et al. Microstructure and mechanical properties of aluminum

- 5083 weldments by gas tungsten arc and gas metal arc welding. *Mater Sci Eng A* [Internet]. Elsevier B.V. 2012; 549:7–13.
3. Atabaki MM, Yazdian N, Kovacevic R. Partial penetration laser-based welding of aluminum alloy (AA 5083-H32). *Opt - Int J Light Electron Opt* [Internet]. Elsevier GmbH. 2016; 127(16):6782–804.
 4. Subbaiah K, Geetha M, Shanmugarajan B. Comparative evaluation of tungsten inert gas and laser beam welding of AA5083-H321. 2012; 37:587–93.
 5. Sanchez-Amaya JM, Delgado T, De Damborenea JJ, Lopez V, Botana FJ. Laser welding of AA 5083 samples by high power diode laser. *Sci Technol Weld Join*. 2009; 14(1):78–86. Crossref
 6. Hirata T, Oguri T, Hagino H, Tanaka T, Wook S, Takigawa Y, et al. Influence of friction stir welding parameters on grain size and formability in 5083 aluminum alloy. 2007; 456:344–9.
 7. Lombard H, Hattingh DG, Steuwer A, James MN. Optimising FSW process parameters to minimise defects and maximise fatigue life in 5083-H321 aluminium alloy. *Eng Fract Mech*. 2008; 75(3–4):341–54. Crossref
 8. Palanivel R, Mathews PK. Prediction and optimization of process parameter of friction stir welded AA5083- H111 aluminum alloy using response surface methodology. 2012; 19(1):1–8.
 9. Gupta R, Zhang R, Davies C, Birbilis N. Influence of Mg content on the sensitisation and corrosion of Al-x Mg (-Mn) alloys. *Corrosion*. 2013; 69(11):1081–7. Crossref
 10. Heidersbach RH, Dexter SC, Griffin RB, Montemarano J. Marine corrosion. *ASM Handbook*. 1987; 13:893–926.
 11. Hossain KMA, Easa SM, Lachemi M. Evaluation of the effect of marine salts on urban built infrastructure. *Build Environ*. 2009; 44(4):713–22. Crossref
 12. Dobrzanski LA, Brytan Z, Grande MA, Rosso M. Corrosion resistance of sintered duplex stainless steels in the salt fog spray test. *J Mater Process Technol*. 2007; 192–193:443–8. Crossref
 13. Vilaca P, Pepe N, Quintino L. Metallurgical and Corrosion Features of Friction Stir Welding of AA5083-H111. *Weld World*. 2013; 50(9–10):55–64.
 14. Miladinov M. Corrosion Behavior of TIG Welded AlMg6Mn Alloy. 2016; 66(2):10–7.
 15. Zucchi F, Trabanelli G, Grassi V. Pitting and stress corrosion cracking resistance of friction stir welded AA 5083. *Mater Corrosion*. 2001; 52(11):853–9. Crossref
 16. Lomolino S, Tovo R, Santos J Dos. On the fatigue behaviour and design curves of friction stir butt-welded Al alloys. *Int J Fatigue*. 2005; 1–6. Crossref
 17. Lombard H, Hattingh DG, Steuwer A, James MN. Effect of process parameters on the residual stresses in AA5083-H321 friction stir welds. *Mater Sci Eng A*. 2009; 501(1–2):119–24. Crossref
 18. N SS, Murugan N, Suresh S. Mathematical Modeling of Ductility of. *Int J Mater Res Electron Electr Syst*. 2011; 11(3):1–4.
 19. ASTM Standard B928/B928M. Standard Specification for High Magnesium Aluminum-Alloy Sheet and Plate for Marine Service and Similar Environments. *ASTM B Stand*. 2009; 1–12.
 20. ASTM Norma G 66. Standard Test Method for Visual Assessment of Exfoliation Corrosion Susceptibility of 5XXX Series Aluminum Alloys (ASSET Test). 2006 Oct; 1–4.
 21. Corro- E. Standard Test Method for Determining the Susceptibility to Intergranular Corrosion of 5XXX Series Aluminum Alloys by Mass Loss After Exposure to Nitric Acid (NAML Test). 2016; 1–10.
 22. Magudeeswaran G, Balasubramanian V, Madhusudhan Reddy G, S Balasubramanian T. Effect of Welding Processes and Consumables on Tensile and Impact Properties of High Strength Quenched and Tempered Steel Joints. *J Iron Steel Res Int*. 2008; 15(6):87–94. Crossref
 23. Birbilis N, Buchheit RG. Electrochemical Characteristics of Intermetallic Phases in Aluminum Alloys An Experimental Survey and Discussion. *J Electrochem Soc*. 2005; 152(4):140–51. Crossref
 24. Choi DH, Ahn BW, Quesnel DJ, Jung SB. Behavior of β phase (Al₃Mg₂) in AA 5083 during friction stir welding. *Intermetallics*. 2013; 35:120–7. Crossref
 25. Moldovan P, Stanica CN, Ciobanu G, Ungureanu I, Iorga GM, Buțu M. Intergranular corrosion of AA 5083 - H321 aluminum alloy. *UPB Sci Bull Ser B Chem Mater Sci*. 2014; 76(3):169–80.
 26. Oguocha INA, Adigun OJ, Yannacopoulos S. Effect of sensitization heat treatment on properties of Al-Mg alloy AA5083-H116. *J Mater Sci*. 2008; 43(12):4208–14. Crossref